

Experimental control of chaos in a laser

M. Ciofini, R. Meucci, and F. T. Arecchi*

Istituto Nazionale di Ottica, 50125 Arcetri, Firenze, Italy

(Received 14 June 1994; revised manuscript received 7 March 1995)

The chaotic behavior of a single-mode laser has been stabilized over different periodic orbits by a small modulation of a control parameter, at a frequency near one of the frequencies still evident above the broad continuum in the chaotic power spectrum. Criteria for selecting the perturbation frequency and evaluating the robustness of the stabilization are given. The main experimental features are reproduced by numerical simulations.

PACS number(s): 05.45.+b, 42.50.Lc, 42.55.Lt

The problem of controlling chaos has received much recent interest. Stabilizing a chaotic dynamics to periodic orbits or steady states by small perturbations opens novel scenarios in the theory and application of nonlinear dynamics. The advantage of dealing with chaotic attractors is that they contain an infinite number of different unstable orbitals [1] and hence provide a large choice.

Different methods have been used for controlling chaos to periodic orbits, based (i) on the determination of the stable and unstable directions in the Poincaré section [2–4], (ii) on a self-controlling feedback procedure [5], (iii) on the introduction of small modulation of a control parameter [6–11], and (iv) on the knowledge of a prescribed goal dynamics [12]. Methods (i) and (ii) are usually called feedback methods while (iii) and (iv) are called non-feedback methods [13].

Regarding case (iii), theoretical work has dealt with the suppression of chaos in the dynamics of different models [6–8]. Although control of chaos by small modulations has not been proved in general, some specific models [7] show the reduction of the leading Lyapunov exponent, thus resulting in the stabilization of weakly unstable periodic solutions. From an experimental point of view, it has been shown that small modulations allow control of chaos in different dynamical systems such as a microwave-pumped spin wave instability [9], a bistable magnetoelastic system [6], electronic circuits [10], and a laser with modulated losses [11]. In particular, Ref. [11] shows that the chaotic attractor of a single-mode CO₂ laser with modulated losses can be stabilized over several different periodic orbits by adjusting the phase of a perturbation at a frequency in the ratio 1:2 or 1:4 with the forcing frequency.

In this paper we show that the chaotic behavior of a laser can be stabilized by a small modulation of a control parameter at a frequency suggested by the power spectrum of the free-running system. Resonant stimulation was already proposed by Hübner and Lüscher to control nonlinear oscillators [12]. In that case, the perturbation vector was calculated as the difference between the goal

dynamics and the actual free-running dynamics. This method has the advantage of taking into account all the information contained in the unperturbed system. However, it cannot be easily implemented, since in general some variables are not directly accessible, and recursion to delay coordinates embedding [14] would make it difficult to apply it in real time. Furthermore, this goal dynamics is not generally implementable by tiny perturbations, but may require corrections of the same order as the main signal.

In our case, robust stabilization of different periodic orbits can be achieved by a parametric perturbation with frequency close to that of the leading cycle embedded in the chaotic attractor and with relative amplitudes of the order of a few percent. Since the perturbation parameters are suggested by a preliminary global measurement on the system itself, this method is intermediate between methods (i), (ii), and (iii). On the one hand, it avoids the on-line tracking of a local feedback stabilization, which may put too stringent requirements on the time resolution of the tracking apparatus. On the other hand, it adapts to a global system property and hence is not imposed as an external artifact. Our experiment consists of a CO₂ laser where chaotic instabilities are induced by a feedback signal with a damping rate comparable to the population decay rate [15,16]. Numerical simulations on a four-level model [17,18] of the CO₂ laser confirm the experimental results.

The experimental apparatus (Fig. 1) consists of a single-mode CO₂ laser with an intracavity loss modulator (electro-optic crystal driven by a voltage V). The optical cavity is 1.35 m long and the total transmission coefficient T is 0.09 for a single pass. The intensity decay rate $\kappa(V)$ can be expressed as [15]

$$\kappa(V) = \frac{c}{2L} \left[2T + (1-2T)\sin^2 \left(\frac{\pi(V-V_0)}{V_\lambda} \right) \right],$$

where $V_\lambda = 4240$ V and $V_0 = 100$ V accounts for a small misalignment between the optical axes of the crystal and the intracavity polarizer. The modulation voltage V is applied through a feedback loop consisting of a detector yielding a current proportional to the laser output intensity plus an amplifier. The feedback voltage V is summed

*Also with the Physics Department, University of Firenze, Firenze, Italy.

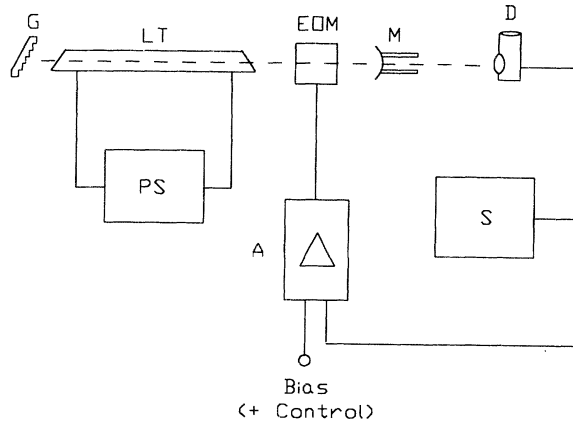


FIG. 1. Experimental setup: G, grating; LT laser tube; EOM, electro-optic modulator; M, mirror; D, detector; S, scope; and A, amplifier. The feedback loop provides the chaotic regime, as described in Ref. [15]; the control is introduced as an external signal to amplifier A.

to a bias B introduced through the second input of the amplifier.

For fixed pump value and amplifier gain, the bias voltage B acts as the control parameter. The system shows a large variety of dynamical behaviors, including chaotic instabilities due to a competition among unstable points leading to heteroclinic orbits [16]. Here, we refer to a range of B values where first a stable point undergoes a Hopf bifurcation and then the limit cycle is destabilized toward chaos through a sequence of subharmonic bifurcations. The experimental sequence is shown in Fig. 2, where the attractors are obtained by plotting the laser intensity I versus the voltage V .

When the system is in the chaotic region, the stabilization of periodic orbits has been obtained by adding to the bias voltage a small sinusoidal perturbation, so that it becomes

$$\tilde{B} = B[1 + \epsilon \sin(2\pi f t)].$$

The experimental results shown in Fig. 3 are obtained with $B = 443$ V and $\epsilon = 0.018$; in case (a) we set $f = 36.0$ kHz, while in case (b) we set $f = 37.0$ kHz. Figure 4 gives the power spectra of the unperturbed laser of Fig. 2(d) and of the perturbed systems of Figs. 3(a) and 3(b). It is important to observe that the unperturbed spectrum [Fig. 4(a)] still contains a peak at frequency $f^* = 38.4$ kHz, which is the remnant of the limit cycle. Therefore, the chaotic attractor of Fig. 2(d) can be stabilized by choosing a frequency f close to f^* , while the relative perturbation amplitude ϵ is of the order of 2%. Moreover, it appears from Figs. 4(b) and 4(c) that the fundamental frequencies of the stabilized attractors are locked to the perturbation frequencies [note that these frequencies are quite different from those of the attractors of Figs. 2(e) and 2(f), reported in the caption]. Once the desired orbit is selected, it lasts for a time on the order of several minutes, until uncontrolled drifts spoil the resonance condition between the cavity mode and the gain line.

For the sake of completeness, we have tested the effect

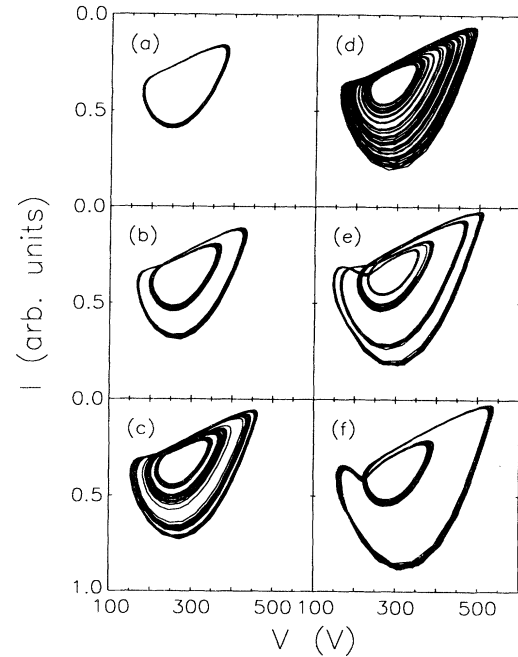


FIG. 2. Experimental phase space plots (laser intensity I vs feedback voltage V) for increasing values of the bias voltage B (we denote with f^* the fundamental frequency): (a) limit cycle at $f^* = 41.4$ kHz, $B = 416$ V; (b) subharmonic bifurcation $f/2$ at $f^* = 40.2$ kHz, $B = 429$ V; (c) subharmonic $f/4$ at $f^* = 39.6$ kHz, $B = 436$ V; (d) chaotic attractor, $B = 443$ V; (e) period-4 limit cycle at $f^* = 35.0$ kHz, $B = 451$ V; (f) period-2 limit cycle at $f^* = 33.5$ kHz, $B = 472$ V.

of perturbations near the first two bifurcation points ($B = 416$ and 429 V). Using a perturbation amplitude such as that applied in the chaotic regime and perturbation frequencies close to the corresponding f^* values, no relevant changes have been detected in the attractors.

The stabilization has been also tested with respect to changes of the amplitude ϵ . Figure 5(a) shows the region in the parameter space (ϵ, f) for which it is possible to

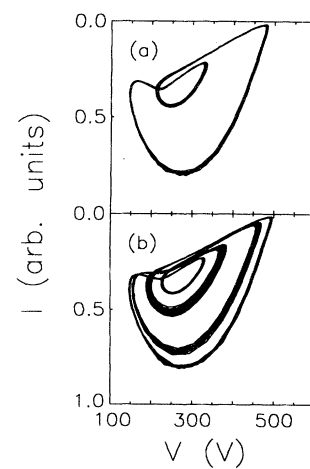


FIG. 3. Stabilized orbits (I vs V) in the chaotic parameter range [Fig. 2(d), $B = 443$ V] with $\epsilon = 0.018$: (a) perturbation frequency $f = 36.0$ kHz; (b) perturbation frequency $f = 37.0$ kHz.

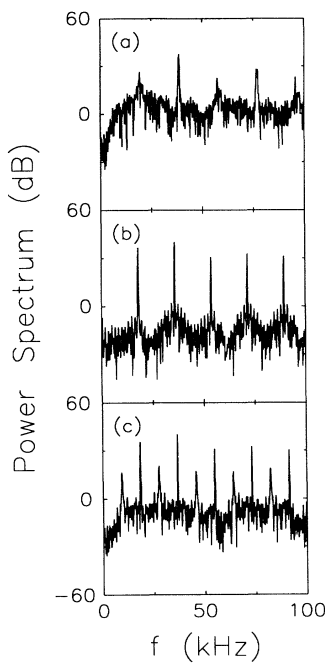


FIG. 4. Power spectra corresponding to (a) the unperturbed chaotic attractor of Fig. 2(d); (b) and (c) the stabilized orbits of periods 2 and 4 of Fig. 3, respectively.

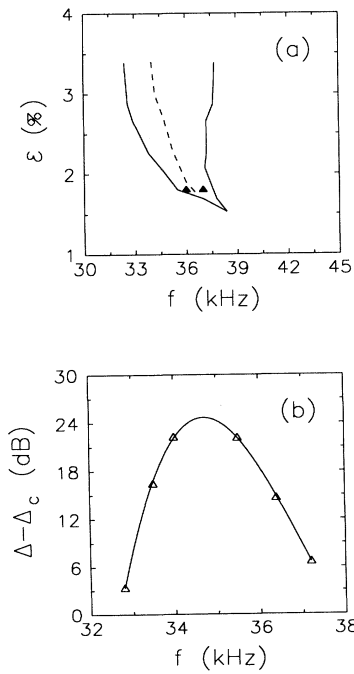


FIG. 5. (a) Experimental stability domain (area between the two solid lines) in the parameter space; the dashed line separates the regions of period-4 and period-2 stable orbits (right side and left side, respectively). (b) Dependence of the robustness indicator $\Delta - \Delta_c$ on the perturbation frequency f , for $\epsilon = 0.027$: symbols denote experimental points (the error bars are included within the symbol size) while the solid line represents a cubic fit.

observe regular behaviors, such as those reported in Fig. 3 (here indicated by full triangles). In order to characterize the robustness of the stabilization, we consider the difference $\Delta = S(f) - \tilde{S}$ between the peak value of the power spectrum $S(f)$ at the fundamental frequency of the stabilized orbit and the averaged spectrum \tilde{S} over the range 0–100 kHz. Δ is a suitable indicator of order, since it is maximum for a regular noiseless signal, while it goes to zero for a broadband featureless spectrum. For the chaotic spectrum of Fig. 4(a) $\Delta_c = 34.0$ dB, while for the stabilized cases of Figs. 4(b) and 4(c), $\Delta = 56.3$ and 47.8 dB, respectively. Figure 5(b) shows the dependence of $\Delta - \Delta_c$ on the perturbation frequency measured at $\epsilon = 0.027$. Thus, the boundaries of Fig. 5(a) correspond to the merging of the peak with the chaotic background, so that Δ reduces to Δ_c . In view of this role, $\Delta - \Delta_c$ can be considered as a convenient “robustness indicator.” The fact that the period-1 stable orbit does not appear is not due to experimental difficulties, but to the position of the stability region. Increasing ϵ over 8%, the stable period-1 cycle can also be obtained, but the shape of the orbit is strongly deformed because the perturbation can no longer be considered small.

We have also found two narrower stability windows around the perturbation frequencies $f_1 = \frac{2}{3}f^*$ and $f_2 = \frac{3}{2}f^*$, even though the first of these frequencies does not emerge from the broad part of the spectrum. These windows, where the system is locked over a periodic orbit with the same frequency of the perturbation, have shapes, which, like Fig. 5(a), resemble the Arnold tongues in a quasiperiodic dynamical system [19].

A meaningful comparison between theory and experiment can be performed introducing, instead of the usual

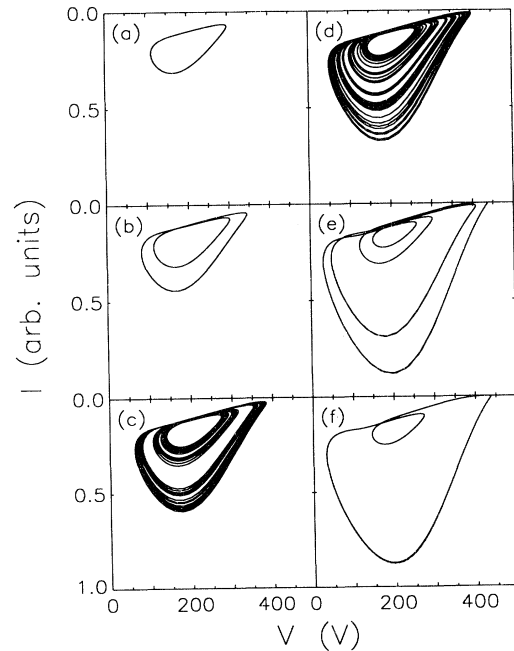


FIG. 6. Numerical simulations (I vs V) for different values of the parameter B : (a) $B = 430$ V; (b) $B = 434$ V; (c) $B = 436$ V; (d) $B = 437$ V; (e) $B = 442$ V; and (f) $B = 444$ V.

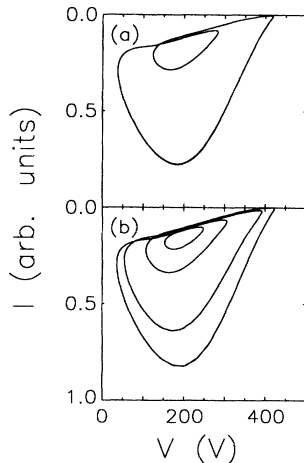


FIG. 7. Stabilized orbits (I vs V) obtained by numerical simulations with $B = 437$ V and $\epsilon = 0.014$: (a) perturbation frequency 37.0 kHz and (b) perturbation frequency 39.0 kHz.

rate equations (two-dimensional model), a more detailed description for the CO_2 dynamics, the so-called four-level model [17]. This improved model, accounting for the coupling between the two laser levels and their rotational manifolds, has also provided quantitative agreement with the experimental data in the case of modulated losses [18]. Choosing a suitable set of model parameters [15,18], we obtain the Hopf transition and the successive destabilization of the limit cycle with B and f^* values close to the experiment (Fig. 6). When adding the sinusoidal perturbation, we obtain ϵ and f ranges close to the experimental ones, as shown in the examples of Fig. 7. Figure 8, which displays the dependence of $\Delta - \Delta_c$ on

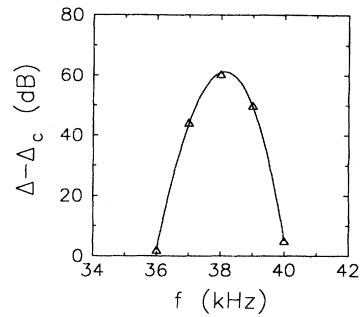


FIG. 8. Robustness of the model: dependence of $\Delta - \Delta_c$ on the perturbation frequency f , for $B = 437$ V, $\epsilon = 0.014$. Symbols denote numerical tests while the solid line represents a cubic fit.

the perturbation frequency ($B = 437$ V, $\epsilon = 0.014$), confirms the validity of the robustness criteria previously introduced.

To conclude, we have tested an experimental method for stabilization of the chaotic attractor of a single-mode CO_2 laser with feedback. The stabilization is obtained by means of small parametric modulations having relative amplitudes of a few percent and frequencies that have ratios of 1:1, 2:3, and 3:2 with respect to the frequency f^* of the leading cycle embedded in the chaotic attractor. We have also characterized, in proximity of f^* (ratio 1:1), the size of the parameter window over which stabilization is achieved. Numerical tests provide a reproduction of the experimental results.

The authors gratefully acknowledge N. B. Abraham for helpful discussions. This work was partly supported by the EC Contract No. SCI*-CT91-0697 (TSTS).

[1] D. Auerbach, P. Cvitanovic, J. P. Eckmann, G. Gunaratne, and I. Procaccia, *Phys. Rev. Lett.* **58**, 2387 (1987); C. Grebogi, E. Ott, and J. A. Yorke, *Phys. Rev. A* **37**, 1711 (1988).

[2] E. Ott, C. Grebogi, and J. A. Yorke, *Phys. Rev. Lett.* **64**, 1196 (1990); W. L. Ditto, S. N. Rauseo, and M. L. Spano, *ibid.* **65**, 3211 (1990); U. Dressler and G. Nitsche, *ibid.* **68**, 1 (1992).

[3] B. Peng, V. Petrov, and K. Showalter, *J. Phys. Chem.* **95**, 4957 (1991).

[4] E. R. Hunt, *Phys. Rev. Lett.* **67**, 1953 (1991); R. Roy, T. W. Murphy, T. D. Maier, Z. Gills, and E. R. Hunt, *ibid.* **68**, 1259 (1992); T. L. Carroll, I. Triandaf, I. Schwartz, and L. Pecora, *Phys. Rev. A* **46**, 6189 (1992).

[5] K. Pyragas, *Phys. Lett. A* **170**, 421 (1992); K. Pyragas and A. Tamaševicius, *ibid.* **180**, 99 (1993); S. Bielawski, D. Derozier, and P. Glorieux, *Phys. Rev. E* **49**, R971 (1994).

[6] R. Lima and M. Pettini, *Phys. Rev. A* **41**, 726 (1990); L. Fronzoni, M. Giocondo, and M. Pettini, *ibid.* **43**, 6483 (1991).

[7] Y. Braiman and I. Goldhirsch, *Phys. Rev. Lett.* **66**, 2545 (1991); R. Chacón and J. Díaz Berjarano, *ibid.* **71**, 3103 (1993).

[8] Y. Liu and J. R. Rios, *Leite, Phys. Lett. A* **185**, 35 (1994).

[9] A. Azevedo and S. M. Rezende, *Phys. Rev. Lett.* **66**, 1342 (1991).

[10] T. Kapitaniak, L. J. Kocarev, and L. O. Chua, *Int. J. Bifurc. Chaos* **3**, 459 (1993).

[11] R. Meucci, W. Gadomski, M. Ciofini, and F. T. Arecchi, *Phys. Rev. E* **49**, R2528 (1994).

[12] A. Hübner and E. Lüscher, *Naturwissenschaften* **76**, 67 (1989); B. B. Plapp and A. Hübner, *Phys. Rev. Lett.* **65**, 2302 (1990).

[13] T. Shinbrot, C. Grebogi, E. Ott, and J. A. Yorke, *Nature (London)* **363**, 411 (1993).

[14] N. H. Packard, J. P. Crutchfield, J. D. Farmer, and R.S. Shaw, *Phys. Rev. Lett.* **45**, 712 (1980).

[15] F. T. Arecchi, W. Gadomski, and R. Meucci, *Phys. Rev. A* **34**, 1617 (1986).

[16] F. T. Arecchi, R. Meucci, and W. Gadomski, *Phys. Rev. Lett.* **58**, 2205 (1987).

[17] R. Meucci, M. Ciofini, and Peng-ye Wang, *Opt. Commun.* **91**, 444 (1992).

[18] M. Ciofini, A. Politi, and R. Meucci, *Phys. Rev. A* **48**, 605 (1993); C. L. Pando L., R. Meucci, M. Ciofini, and F. T. Arecchi, *Chaos* **3**, 279 (1993).

[19] V. I. Arnold, *Trans. Am. Math. Soc.* **42**, 213 (1965).